

**SYNTHESIS OF SILICA NANOCOLLOIDS DRUG DELIVERY SYSTEM BY
MICELLE FORMATION APPROACH**

HAJARUL AZWANA BINTI AB WAB

UNIVERSITI SAINS MALAYSIA

2013

**SYNTHESIS OF SILICA NANOCOLLOIDS DRUG DELIVERY SYSTEM BY
MICELLE FORMATION APPROACH**

By

HAJARUL AZWANA BINTI AB WAB

**Thesis submitted in fulfillment of the requirements
for the degree of
Master of Science**

OCTOBER 2013

DECLARATION

I hereby declare that I have conducted, completed the research work and written the dissertation entitled “Synthesis of Silica Nanocolloids Drug Delivery System by Micelle Formation Approach”. I also declare that it has not been previously submitted for the award of any degree or diploma or other similar title of this for any other examining body or University.

Name of student: Hajarul Azwana Ab Wab

Signature:

Date: 27 September 2013

Witness by

Supervisor: Assoc. Prof. Dr. Khairunisak Abdul Razak

Signature:

Date: 27 September 2013

ACKNOWLEDGEMENTS

First of all, I would like to express my special gratitude to my supervisor Associate Professor Dr Khairunisak Abdul Razak for her continuous supervision, guidance and support from the initial to the final stage of my research. I believe I am not able to finish my project without the help, patience and valuable advices from her. My sincere gratitude also goes to my co-supervisors; Assoc. Prof. Dr. Azlan Abdul Aziz and not to forget to Assoc. Prof. Dr. Shaharum Shamsuddin for their insightful ideas and suggestions throughout this research work. All of them have guided me in a scientific way to conduct a research with their profound knowledge and research experience.

I also wish to extend my thanks to Universiti Sains Malaysia through Research University Postgraduate Research Grant Scheme (RUPRGS) and Graduate Assistant Scheme (GA). Also not to forget to MyBrain15 programs which gave me MyMaster scholarship. I would like to thank all technicians in School of Materials and Mineral Resources Engineering and INFORMM who helped me a lot especially Mrs. Dyana and Madam Fong. Besides, I would like to express my appreciation to my best friends Mrs. Rabizah, Ms. Syafinaz, Mr. Navan, Ms. Ng Soo Ai, Ms. Hashimah and Ms. Ng Chai Yan for sharing my laughs and tears. Finally, I would like to express my deepest gratitude to my family for encouragement and always pray for my success.

Thank you.

TABLE OF CONTENTS

	Page
TITLE	i
DECLARATION	ii
ACKNOWLEDGEMENT	iii
TABLE OF CONTENTS	iv
LIST OF TABLES	ix
LIST OF FIGURES	xii
LIST OF ABBREVIATIONS	xx
LIST OF SYMBOLS	xxv
LIST OF PUBLICATIONS	xxvi
ABSTRAK	xxvii
ABTRACT	xxviii
CHAPTER 1: INTRODUCTION	
1.1 Research background	1
1.2 Problem statement	3
1.3 Objectives	5
1.4 Thesis scope	5
CHAPTER 2: LITERATURE REVIEW	
2.1 Introduction	6
2.2 Silica nanoparticles (NPs)	7
2.2.1 Properties of Silica	9
2.2.2 Structure of Silica NPs	11

2.2.3 Silica surface properties	13
2.2.3.1 Adsorption of organic molecules on silica surface	15
2.2.3.2 Surface functionalization of silica	17
2.3 Synthesis and fabrication of Silica NPs	17
2.3.1 Sol-Gel process	18
2.3.1.1 Stöber process	20
2.3.2 Hydrothermal growth method	22
2.3.3 Ionic liquid template	24
2.3.4 Microemulsion	25
(a) Water in Oil microemulsion (W/O) or reverse micelle	27
(b) Oil in Water microemulsion (O/W)	29
(c) Micelle formation	30
2.4 Parameters of synthesis method	31
2.4.1 Stirring rate	31
2.4.2 Reaction temperature	32
2.4.3 Amount of alcohol (co-solvent/co-surfactant)	35
2.4.4 Different types of alcohol	38
2.4.5 Different types of Si precursor	39
2.4.6 Amount of Si precursor	41
2.4.7 Type of surfactant	43
2.4.7.1 Cationic surfactant	44
2.4.7.2 Anionic surfactant	45
2.4.7.3 Non-ionic surfactant	45
2.4.8 Amount of surfactant	49
2.5 Application of Silica NPs	51

2.5.1 Photodynamic therapies	51
2.5.2 Drug delivery system	53
2.5.2.1 Drug loading	55
2.5.2.2 Drug release	58
2.5.2.3 Stability in colloidal suspension	58
2.5.2.4 Degradation	62
2.5.2.5 <i>In vitro</i> cytotoxicity	64
2.5.2.6 Biodistribution, biocompatibility and clearance	67
2.6 Tuberculosis disease	69
2.7 Summary of literature review	72
 CHAPTER 3: METHODOLOGY	
3.1 Introduction	73
3.2 Chemical and materials	73
3.2.1 Synthesis of silica NPs colloids by micelle formation approach	75
3.2.2 Synthesis of silica NPs colloids with Isoniazid (water soluble drug)	79
3.2.3 Synthesis of silica NPs colloids with Rifampicin (poorly water soluble drug)	80
3.3 Preparation of silica NPs colloids mixture with biocoating (excipient addition)	81
3.4 Stability study of SiRIF NPs colloids	82
3.5 Drug release study	84
3.5.1 Phosphate Buffer Solution concentration (PBS)	85

3.5.2 Different pH	85
3.6 Toxicity test	85
3.7 Samples characterization	87
3.7.1 Morphology observation	87
3.7.2 Concentration of drugs determination	87
3.7.3 Hydrodynamic particle size and zeta potential determination	90
3.7.4 X-ray diffraction (XRD)	91
3.7.5 Toxicity analysis by Elisa microplate Spectrophotometer	91
 CHAPTER 4: RESULTS AND DISCUSSIONS	
4.1 Introduction	93
4.2 Synthesis of silica NPs colloids	94
4.2.1 Micelles structure formation	94
4.2.2 Silica NPs colloids formation	95
4.3 Synthesis of silica NPs entrapped Isoniazid colloids (SiINH) DDS	99
4.3.1 The effect of reaction temperature	199
4.3.2 The effect of volume of Si precursor	103
4.3.3 The effect of volume of 2-butanol	106
4.3.4 The effect of amount of Tween 80 surfactant	108
4.3.5 The effect of amount of Isoniazid	113
4.4 Synthesis of silica NPs colloids entrapped Rifampicin (SiRIF)	117
4.4.1 The effect of reaction temperature	118
4.4.2 The effect of volume of 2-butanol	123
4.4.3 The effect of amount of Tween 80 surfactant	125

4.4.4 the effect of amount of Rifampicin	129
4.4.5 Effects of parameter involved on Rifampicin and filtration efficacy of SiRIF	131
4.5 Zeta potential of silica NPs colloids entrapped Rifampicin (SiRIF)	134
4.6 Stability of silica NPs entrapped Rifampicin (SiRIF) colloids	137
4.6.1 Sodium chloride (NaCl)	137
4.6.2 Mouse serum media	140
4.7 Drug release study	142
4.7.1 Different PBS concentration	143
4.7.2 Different pH	144
4.8 Toxicity test	149
CHAPTER 5: CONCLUSIONS AND SUGGESTIONS FOR FUTURE WORK	
5.1 Conclusions	153
5.2 Suggestions for future work	154
REFERENCES	155
APPENDIX	172

LIST OF TABLES

	Page
Table 2.1:	Physical and chemical properties of different amorphous silica 11
Table 2.2:	Summary of surfactant used to produced silica NPs 47
Table 2.3:	Typical drug loading methods 57
Table 2.4:	Degradation study of silica NPs 63
Table 2.5:	In vitro toxicity on silica NPs 65
Table 2.6:	Biodistribution and clearance of silica based NPs in mice 68
Table 3.1:	Materials and chemicals used in this study 74
Table 3.2:	Parameters study of synthesis of silica NPs colloids with Isoniazid 79
Table 3.3:	Parameters study of synthesis of silica NPs colloids with Rifampicin 80
Table 4.1:	Hydrodynamic size and polydispersity index (PDI) of micelles structure with varying temperature 95
Table 4.2:	Hydrodynamic size and polydispersity index (PDI) of silica NPs colloids formation after addition of Si precursor 97
Table 4.3:	The effects of reaction temperature on the SiINH. Mean particle size was obtained from TEM images while hydrodynamic sizes and PDI values were obtained from zetasizer 101
Table 4.4:	The effect of volume of Si precursor on SiINH. Mean particle size was obtained from TEM images while hydrodynamic sizes and PDI values were obtained from zetasizer 105
Table 4.5:	The effects of volume of 2-butanol on SiINH. Mean particle size was obtained from TEM images while hydrodynamic sizes and PDI values were obtained from zetasizer 108
Table 4.6:	The effect of amount of surfactant Tween 80 on SiINH. Mean particle size was obtained from TEM images while hydrodynamic sizes and PDI values were obtained from zetasizer 111

Table 4.7:	Effect of amount of Tween 80 on concentration of SiINH before synthesis, after synthesis, after dialysis and after re-concentration	113
Table 4.8:	The effect of amount of Isoniazid on SiINH. Mean particle size was obtained from TEM images while hydrodynamic sizes and PDI values were obtained from zetasizer	115
Table 4.9:	Effect of initial amount of Isoniazid on concentration of SiINH before synthesis, after synthesis, after dialysis and after re-concentration	116
Table 4.10:	The effects of reaction temperature on SiRIF. Mean particle size was obtained from TEM images while hydrodynamic sizes and PDI values were obtained from zetasizer	121
Table 4.11:	The effects of volume of 2-butanol on SiRIF. Mean particle size was obtained from TEM images while hydrodynamic sizes and PDI values were obtained from zetasizer	125
Table 4.12:	The effects of Tween 80 surfactant on SiRIF. Mean particle size was obtained from TEM images while hydrodynamic sizes and PDI values were obtained from zetasizer	128
Table 4.13:	The effects of Rifampicin amount on SiRIF. Mean particle size was obtained from TEM images while hydrodynamic sizes and PDI values were obtained from zetasizer	131
Table 4.14:	Summary of concentration and filtration efficacy of SiRIF with different synthesis parameters	133
Table 4.15:	Isoelectric point of SiRIF with varying temperature	137
Table 4.16:	Filtration efficacy of 50 nm SiRIF in different concentration of NaCl solution	139
Table 4.17:	Filtration efficacy of 70 nm SiRIF in different concentration of NaCl solution	140
Table 4.18:	Filtration efficacy of 50 nm SiRIF in different vol.% of mouse serum media	142
Table 4.19:	Filtration efficacy of 70 nm SiRIF in different vol. % mouse serum media	142
Table 4.20:	Cumulative release of SiRIF in 0.1 mM PBS (pH 7.4)	143
Table 4.21:	Cumulative release of 1.0 mM Rifampicin in different pH condition	147

Table 4.22:	Cumulative release of 50 nm and 70 nm SiRIF in 1.0 mM PBS with varying pH	148
Table 4.23:	IC ₅₀ value of 20 nm and 40 nm blank silica NPs in osteosarcoma cells	150
Table 4.24:	IC ₅₀ value of 50 nm and 70 nm SiRIF in osteosarcoma cells	152

LIST OF FIGURES

Figure 2.1:	Various forms of silica	8
Figure 2.2:	Schematic diagrams of amorphous silica structures and reaction on its surface	10
Figure 2.3:	(A) Transmission electron microscope (TEM) images of nonporous silica (Stöber), mesoporous silica (Meso S), mesoporous silica nanorods with aspect ratio 2 (AR2), and mesoporous silica nanorods with aspect ratio 8 (AR8) and High resolution TEM (HRTEM) image of a nanoparticle from Meso S; scale bars = 200 nm except in high-resolution image = 50 nm	12
Figure 2.4:	The formation of silanol groups on the silica surface: (a) Condensation polymerization; (b) Rehydroxylation	14
Figure 2.5:	Types of silanol groups and siloxane bridges on the surface of amorphous silica, and internal (OH ⁻) groups. Q ⁿ terminology is used in NMR, where n indicates the number of bridging bonds (-O-Si) tied to the central Si atom: Q ⁴ , surface siloxanes; Q ³ , single silanols; Q ² , geminal silanols (silanediols)	15
Figure 2.6:	General schematic diagram of silica synthesis processes	18
Figure 2.7:	The stages of silica sol-gel materials synthesis	19
Figure 2.8:	Electron microscopy images of monodispersed silica NPs with various size ranges; (a) seed 18.5 ± 0.8 nm produced by the single stage growth, (b) the one stage regrowth seed 45.5 ± 1.3 nm, (c) the two stage regrowth seed 84 ± 2 nm, (d) three stage regrowth seed 117 ± 2.5 nm, (e) the four stage regrowth seed 141 ± 2.5 nm and (f) the five stage regrowth seed	22
Figure 2.9:	TEM images of silica NPs produced by using different surfactants; (a) cetyl trimethyl ammonium bromide (CTAB), (b) Tergitol, (c) Sodium lauryl sulfate (SCS) and (d) polyethylene glycol (PEG)	23
Figure 2.10:	TEM images of C _n MIM-MSN materials. (a) C ₁₄ MIM-MSN, (b) C ₁₆ MIM-MSN, (c) C ₁₈ MIM-MSN, and (d) C ₁₄ OCMIM-	25

MSN

Figure 2.11:	Hypothetical phase regions of microemulsion systems	27
Figure 2.12:	TEM micrographs showing the Ru(bpy) dye doped silica NPs prepared in different microemulsion systems: (a) NP-5/cyclohexane/water (14 ± 2 nm); (b) AOT/heptane/water (29 ± 8 nm); (c) mixture, AOT + NP-5/heptane/water (130 ± 8 nm)	29
Figure 2.13:	TEM micrographs of mesoporous silica NPs with varying volume of octane: (a) 6 ml, (b) 27 ml and (c) 45 ml	30
Figure 2.14:	FE-SEM images of the silica nanospheres synthesized with various stirring rates: (a) 0 (static condition), (b) 150, (c) 550, and (d) 950 rpm. Scale bar: 100 nm	32
Figure 2.15:	TEM images of mesoporous silica NPs synthesized at different temperatures of: (a) 30 °C, (b) 50 °C and (c) 70 °C	33
Figure 2.16:	SEM images of effect of low reaction temperature on the synthesis of silica NPs: (A) -5 °C and (B) 0 °C	34
Figure 2.17:	Typical SEM images of the as-prepared particles obtained at reaction temperatures of (a) Room temperature (27 °C), (b) 40 °C, (c) 60 °C, and (d) 80 °C. Each sample reveals (a) 2.5, (b) 2.2, (c) 1.7, and (d) 1.6 μ m diameters. The 10 g amount of MPTMS precursor was used	35
Figure 2.18:	TEM micrographs of the samples synthesized at different PT volume percentages: (A) PT-1; 0%, (B) PT-2; 1%, (C) PT-3; 2%, (D) PT-4; 3%, (E) PT-5; 4%, (F) PT-6; 12%, (G) PT-7; 20%, (H) PT-8; 40% and (I) Particle size dependent on PT volume. The scale bars of A, B, C, D, E, F, G and H correspond to 100 nm, 500 nm, 100 nm, 200, 50 nm, 100 nm, 200 nm and 100 nm, respectively	37
Figure 2.19:	SEM images of silica nanospheres prepared with (a) methanol, (b) ethanol, (c) propanol and (d) butanol	39
Figure 2.20:	SEM images of silica NPs synthesized with (a) TMOS, (b) TEOS, (c) TPOS and (d) TBOS	40
Figure 2.21:	SEM images of highly monodisperse silica particles modified	42

with thiol organic groups. The samples were prepared using (A) 1g of MPTMS, (B) 10 g of MPTMS, and (C) 20 g of MPTMS in 100 g of aqueous solution, and the reaction was conducted at room temperature

Figure 2.22:	(A) SAXRD patterns of silica nanoparticels with different surfactant ; (a) CTAB, (b) SDBS and (c) Triton, and TEM images of silica NPs with different surfactant: (B) CTAB, (C) SDBS and (D) Triton. The scale bars of B, C and D correspond to 50 nm, 0.2 mm and 0.2 mm, respectively	44
Figure 2.23:	The schematic illustration of silica formation using CTAB (cationic) and Pluronic F127 (non-ionic) surfactant	50
Figure 2.24:	TEM images of silica with different amount of SDBS concentration; (A) 0.1 M, (B) 0.2 M, (C)) 0.3 M, (D)) 0.4 M, (E) 0.5 M, (F) 0.7 M and (G) 1.0 M	50
Figure 2.25:	Principle stages of photodynamic therapy. Photosensitizer (in syringe or tube) is applied locally or systematically (Stage I), accumulates in tumors (Stage II) and is then activated by external illumination (Stage III). This induces cell damage and death (Stage IV)	52
Figure 2.26:	Photodynamic therapy schematic of HA-silica NPs	53
Figure 2.27:	Various types of nanoparticles used in biomedical research and drug delivery	54
Figure 2.28:	Schematic diagram of nanomatrix structure of fenofibrate, pH-sensitive polymethylacrylate, and mesoporous silica	56
Figure 2.29:	Schematic diagram depicting the synthesis and purification of HPPH-doped silica-based NPs in a micellar medium	57
Figure 2.30:	Hydrodynamic size distribution of 1 mg/ml Mesoporous silica size 42 nm removal of surfactant by centrifuge (MS-42-c), Mesoporous silica size 42 nm removal of surfactant by dialysis MS42-d, and Mesoporous silica size 42 nm coated with PEG, hydrothermal treatment and removal of surfactant by centrifuge MS42@PEG-hy-c NPs measured by DLS at RT in various media: (a) D.I. H ₂ O, (b) PBS, and (c) DMEM + 10% FBS. Long-term colloidal stability of (d) MS42-d and (e) MS42@PEG-hy-c NPs in various media at RT and 37 °C.	60

Data represent mean \pm SD from three independent experiments. Inset: a photograph of MS42@PEG-hy-c colloidal solutions after 10 days aging in D.I. H₂O, PBS, and DMEM + 10 % FBS at 37 °C

Figure 2.31:	(a) TEM images of Ludox TM50 spherical silica NPs, (b) Particle size and zeta potential for suspension of Ludox TM50 (1 wt %) at different NaCl concentrations, (c) Particle size distributions in NaCl, (d) Average particle size in BSA and (e) TEM picture of silica in BSA (agglomerate)	61
Figure 2.32:	Variation in the TEM images of colloidal mesoporous silica (CMPS) 80 nm with the immersion time in PBS: (a) 0, (b) 1, (c) 2, (d) 3, (e) 4, (f) 5 days, (g) Variation in the appearances of CMPS 80 nm with the immersion time in PBS and (h) Schematic diagram of degradation of CMPS with a dialysis	63
Figure 2.33:	(a) Clearance of Fluorophore dye conjugated ORMOSIL injected intravenously into the mice (upper panel) and a comparison with the free fluorophore dye injected mice as control (lower panel) at same time	68
Figure 2.34:	Cumulative release of Tuberculosis drug in microemulsion (ME): (a) Different drug in microemulsion and (b) Rifampicin microemulsion release in different pH condition	71
Figure 2.35:	Showing the probable location of all the three drugs in Tween 80 microemulsion system	71
Figure 3.1:	Experimental set-up of synthesis process	76
Figure 3.2:	Synthesis step involves	77
Figure 3.3:	The general flowchart of synthesis process	78
Figure 3.4:	Re-concentration process set up	82
Figure 3.5:	Flowchart of stability test	83
Figure 3.6:	Diagrams of drug release study parameters	84
Figure 3.7:	General flowchart of <i>in vitro</i> toxicity	86
Figure 3.8:	General procedure to seed cell and samples in 96 well plate	86

Figure 3.9:	Figure 3.7: Graph of UV-Vis absorbance for Isoniazid with different concentration	88
Figure 3.10:	Isoniazid calibration curve	89
Figure 3.11:	Graph of UV-Vis absorbance for Rifampicin with different concentration	89
Figure 3.12:	Rifampicin calibration curve	90
Figure 4.1:	Hydrodynamic size distribution for micelles size with varying temperature	95
Figure 4.2:	Hydrodynamic size distribution for silica NPs colloids formation after addition of Si precursor	96
Figure 4.3:	Blank silica NPs colloids synthesized at 50 °C: (a) TEM image and (b) Histogram of particle size distribution	97
Figure 4.4:	XRD spectrum of blank silica NPs colloids	97
Figure 4.5:	Schematic diagram of blank silica NPs colloids formation using micelles formation approach	98
Figure 4.6:	TEM images and histograms of particle size distribution of SiINH at different reaction temperatures: (a) 38 °C, (b) 50 °C and (c) 70 °C	100
Figure 4.7:	Hydrodynamic size distribution of SiINH with varying reaction temperature	101
Figure 4.8:	XRD spectra of SiINH with varying reaction temperature: (a) 38 °C, (b) 50 °C and (c) 70 °C	102
Figure 4.9:	XRD spectrum of Isoniazid drug	102
Figure 4.10:	TEM images and histograms of particle size distribution of SiINH with different volumes of Si precursor: (a) 2 ml, (b) 4 ml, (c) 6 ml and (d) 8 ml	104
Figure 4.11:	Hydrodynamic size distribution of SiINH with varying volume of Si precursor	105

Figure 4.12:	XRD spectra of SiINH with varying volume of Si precursor	106
Figure 4.13:	TEM images and histograms of particle size distribution of SiINH with varying volume of 2-butanol: (a) 6 ml, (b) 10 ml, (c) 14 ml and (d) 18 ml	107
Figure 4.14:	Hydrodynamic size distribution of SiINH with varying volume of 2-butanol	108
Figure 4.15:	TEM images and histograms of particle size distribution of SiINH with different amount of surfactant: (a) 4.0 g, (b) 5.5 g, (c) 7.0 g and (d) 9.0 g	110
Figure 4.16:	Hydrodynamic size distribution of SiINH with different amount of Tween 80	111
Figure 4.17:	Uv-Vis spectrophotometer of SiINH: (a) 4.0 g, (b) 5.5 g, (c) 7.0 g and (d) 9.0 g	112
Figure 4.18:	TEM images and histograms of particle size distribution of SiINH with different amount of Isoniazid: (a) 0.078 g, (b) 0.156 g, and (c) 0.234 g	114
Figure 4.19:	Hydrodynamic size distribution of SiINH with different amount of Isoniazid drug	115
Figure 4.20:	UV-Vis spectra of SiINH with varying amount of Isoniazid: (a) 0.078g, (b) 0.156 g and (c) 0.234 g	116
Figure 4.21:	Schematic diagram of formation of SiINH	117
Figure 4.22:	Schematic diagram of formation of SiRIF	118
Figure 4.23:	TEM images and histograms for distribution of SiRIF with varying reaction temperature: (a) 25 °C, (b) 38 °C, (c) 50 °C and (d) 70 °C	120
Figure 4.24:	Hydrodynamic sizes of SiRIF with varying reaction temperature	121
Figure 4.25:	XRD spectra of SiRIF with varying reaction temperature: (a) 25 °C, (b) 38 °C, (c) 50 °C and (d) 70 °C	122
Figure 4.26:	XRD spectrum of Rifampicin drug	122

Figure 4.27:	TEM images and histograms for distribution of SiRIF with different 2-butanol volume: (a) 6 ml, (b) 10 ml, (c) 12 ml, (d) 14 ml and (e) 18 ml	124
Figure 4.28:	Hydrodynamic distribution of SiRIF with different 2-butanol volume: (a) 6 ml, (b) 10 ml, (c) 12ml, (d) 14 ml and (e) 18 ml	125
Figure 4.29:	TEM images and histograms for distribution of SiRIF with different amount of Tween 80 surfactant: (a) 4.0 g, (b) 5.5 g, (c) 7.0 g and (d) 9.0 g	127
Figure 4.30:	Hydrodynamic distribution of SiRIF with varying amount of Tween 80 surfactant: (a) 4.0 g, (b) 5.5 g, (c) 7.0 g and (d) 9.0 g	128
Figure 4.31:	XRD spectra of SiRIF with varying amount of Tween 80 surfactant: (a) Tween 80 only, (b) 4.0 g, (c) 5.5 g, (d) 7.0 g and (e) 9.0 g	129
Figure 4.32:	TEM images and histograms for distribution of SiRIF with different amount of surfactant: (a) 0.084 g and (b) 0.168 g	130
Figure 4.33:	Hydrodynamic distribution of SiRIF at different amount of surfactant: (a) 0.084 g, (b) 0.168 g	130
Figure 4.34:	Zeta potential of SiRIF in pH1-11: (a) 50 nm and (b) 70 nm	135
Figure 4.35:	Zeta potential of SiRIF with varying temperature: (a) 50 nm and (b) 70 nm	136
Figure 4.36:	UV-Vis spectra of 50 nm SiRIF in NaCl solution: (a) Water, (b) 0.1 M, (c) 0.5 M, (d) 1.0 M	138
Figure 4.37:	UV-Vis spectra of 70 nm SiRIF in NaCl solution: (a) Water, (b) 0.1 M, (c) 0.5 M and (d) 1.0 M	139
Figure 4.38:	UV-Vis spectra 50 nm SiRIF in mouse serum media: (a) Water, (b) 5 %, (c) 10 % and (d) 25 %	141
Figure 4.39:	UV-Vis spectra of 70 nm SiRIF in mouse serum media: (a) Water, (b) 5 %, (c) 10 % and (d) 25 %	141
Figure 4.40:	Cumulative release of SiRIF in 0.1 mM PBS (pH 7.4)	143

Figure 4.41:	Cumulative release in 1.0 mM PBS with varying pH: (a) naked Rifampicin, (b) 50 nm SiRIF and (c) 70 nm SiRIF	146
Figure 4.42:	Color changes of Rifampicin during drug release study with varying pH of the release media	147
Figure 4.43:	50 nm SiRIF after 6 days in PBS with varying pH	149
Figure 4.44:	Toxicity result of naked Rifampicin	150
Figure 4.45:	Toxicity results of blank silica NPs size 20 nm and 40 nm.	150
Figure 4.46:	Toxicity results of SiRIF in osteosarcoma cells: (a) 50 nm and (b) 70 nm	152

LIST OF ABBREVIATIONS

Abbreviation	Compound
(¹ O ₂)	Singlet oxygen
≡Si-O-Si≡	Siloxane
2D	2 dimensional
3T3	Swiss albino mouse fibroblast cells
A549	human bronchoalveolar carcinoma cells
AOT	sodium bis(2-ethylhexyl) sulfosuccinate
APMS	3-aminopropyltrimethoxysilane
APTES	3-aminopropyltriethoxysilane
AR	Aspect ratio
Ba ²⁺	Barium ion
BaCl ₂	Barium chloride
BmimBF ₄	1- butyl-3-methylimidazolium tetrafluoroborate
Brij-56	Polyoxyethylene (10) cetyl ether
BSA	Bovine Serum Albumin
C ₁₄ MIMBr	1-tetradecyl-3- methylimidazolium bromide
C ₁₄ OCMIMCl	1-tetradecyloxymethyl-3-methylimidazolium chloride
C ₁₆ MIMBr	1-hexadecyl-3- methylimidazolium bromide
C ₁₈ MIMBr	1-octadecyl-3-methylimidazolium bromide
Ca ²⁺	Calcium ion
CaCl ₂	Calcium chloride
CaCO ₃	Calcium carbonate
CCD-966sk	human skin normal cell
CMC	Critical micelles concentration
CMPS	colloidal mesoporous silica
CTAB	Cetyltrimethyl ammonium bromide
DDS	Drug delivery system
di-C ₁₂ DMAB	Di-dodecyldimethylammonium bromide
DLS	Dynamic light scattering
DMEM	Dulbecco's Modified Eagle Media
DTAB	Dodecyltrimethylammonium bromide

DY776	3-(3-carboxypropyl)-2-[5-(9-ethyl-6,8,8-trimethyl-2-phenyl-8,9-dihydropyrano[3,2-g]quinolin-1-ium-4-yl)penta-2,4-dien-1-ylidene]-3-methyl-1-(3-sulfonatopropyl)indoline-5-sulfonate
FBS	Fetal Bovine Serum
FESEM	Field emission scanning electron microscope
FITC	Fluorescein isothiocyanate
H ₂ O	Water
HA	Hypocrellins A
HAS	Human serum protein
HCl	Hydrochloric acid
HEK293	human embryonic kidney cells
HPPH	2-devinyl-2-(1-hexyloxyethyl) py-ropheophorbide
HRTEM	High resolution transmission electron microscope
HT-29	human colorectal adenocarcinoma cell (colon)
IC50	the concentration of drugs required to reduce cell growth by 50 %
IEP	Isoelectric point
II-14-3	trimethylene-di(tetradecacyloxyethyl-dimethylammoniumbromide)
IL	Ionic liquid
INH	Isoniazid
IV	Intravenous
J774	Macrophage cells
Ludox TM50	50 wt. % of silica suspension in water
MCM 41	Mobil Catalytic Materials Number 41
Mg ²⁺	Magnesium ion
MgCl ₂	Magnesium chloride
MHSNS	Mesoporous hollow silica nanoparticles
Min-U-Sil	High quality crystalline silica
MKN-28	human adenocarcinoma cell (gastric)
MPT-2	autotitration
MPTMS	3-mercaptopropyl trimethoxysilane

MRC-5	human lung normal cell
MS42@PEG	Mesoporous silica size 42 nm coated with PEG
MS-42-c	Mesoporous silica size 42 nm removal of surfactant by centrifuge
MS42-d	Mesoporous silica size 42 nm removal of surfactant by dialysis
MSNs	Mesoporous silica nanoparticles
MTT	(3-(4,5-dimethylthiazol-2-yl)- 2,5-diphenyltetrazoliumbromide)
Na ⁺	Sodium ion
NaCl	Sodium chloride
NaOH	Sodium hydroxide
NH ₃	Ammonia
NH ₄ OH	Ammonium
NIR	Near infra red
NLR	Long rod nanoparticles
NP5	polyoxyethylene (5) nonylphenylether
NPs	Nanoparticles
NSR	Short rod nanoparticles
O/W	Oil in Water
OD	Optical density
OH ⁻	Hydroxyl ion
ORMOSIL	Organically modified silica
PBS	Phosphate buffer solution/saline
PC12	pheochromocytoma cells
PDI	polydispersity index
PDT	Photodynamic therapy
PEG	Polyethylene glycol
PEO	Polyethylene oxide
PLGA	Poly(lactic-co-glycolic)
PS	Polystyrene
PT	Propane-triol
PTMS	Phenyltrimethoxysilane

PZA	Pyrazinamide
Q ⁿ	Number of bridging bonds
RAW264.7	Murine macrophage cell line
RIF	Rifampicin or Rifampin
ROH	Alcohol
ROS	Reactive oxygen species
RT	Room temperature
RTIL	Room temperature ionic liquid
Ru(bpy)	Ruthenium-tris(2,2'-bipyridyl) dichloride
Sar-Na	N-lauroylsarcosine sodium
SAXRD	Small angle X-ray diffraction
SBA-15	Santa Barbara Amorphous -15
SBF	Simulated body fluid
SD	Standard deviation
SDBS	Sodium dodecylbenzene sulphonate
SEM	Scanning electron microscope
=Si(OH) ₂	Silanediols or geminal silanols
Si(OH) ₄	Silicic acid
Si(OR) ₄	Silica precursor
Si≡OH	Silanol group
Si-Cl	Silica chlorination
SiINH	Silica nanoparticles colloids entrapped Isoniazid
SiRIF	Silica nanoparticles colloids entrapped Rifampicin
SLS	Sodium lauryl sulfate
TB	Tuberculosis
TBOS	Tetrabutyl orthosilicates
TEL	Telmisartan
TEM	Transmission electron microscope
TEOS	Tetraethyl orthosilicates
TMOS	Tetramethyl orthosilicates
TPOS	Tetrapropyl orthosilicates
TRIS	tris- (hydroxymethyl) aminomethane
TSBN	4-(trieth- oxysilyl)butyronitrile

TSTMP	trisodium trimetaphosphate
Tween 80	Polysorbate 80
UV-Vis	UV visible spectrophotometer
VTES	Vinyltriethoxysilane
VTMS	Vinyltrimethoxysilane
W/O	Water in Oil
WS1	human skin normal cell
WST-1	2-(4-Iodophenyl)-3-(4-nitrophenyl)-5-(2,4-disulfophenyl)-2H-tetrazolium
XRD	X-ray diffractometer
XS52	Langerhans cells
XTT	2,3-bis-(2-methoxy- 4-nitro-5-sulfophenyl)-2H-tetrazolium-5-carboxanilide

LIST OF SYMBOL

nm	Nanometer
μm	micrometer
mm	milimeter
l	liter
ml	mililiter
μl	microliter
g	gram
μg	microgram
λ	Wavelength
$^{\circ}\text{C}$	Degree Celcius
$^{\circ}$	Degree
θ	theta
d	diameter
M	Molarity
v/v	Volume per volume
wt	weight
%	percent
h	hour
min	minute
rpm	Revolutions per minute
ζ	potential
\pm	Plus minus

LIST OF PUBLICATIONS

Hajarul, A. A. W., Zakaria, N. O. R. D., Aziz, A. A, & Razak, K. A. (2012). Properties of amorphous silica entrapped Isoniazid drug delivery system. *Advanced Materials Research*, 364, 134-138.

Hajarul, A. A. W., Razak, K. A., Zakaria, N. O. R. D., & Aziz, A. A. (2013). The effect of amount of surfactant and types of drug on amorphous silica drug delivery system (DDS). *Advanced Materials Research*, 620, 112–116.

Shaharum Shamsuddin, Khairunisak Abdul Razak, Venugopal Balakrishnan, and **Hajarul Azwana Ab Wab**. In vitro evaluation of cytotoxicity of colloidal amorphous silica nanoparticles designed for drug delivery on human cell lines. *Journal of Nanomaterials*. In Press.

Hajarul Azwana Ab Wab, Khairunisak Abdul Razak, and Nor Dyana Zakaria. Properties of amorphous silica nanoparticles colloid drug delivery system synthesized using the micelle formation method, submitted to *Journal of Nanoparticle Research* .

SINTESIS SISTEM PENGHANTARAN UBAT NANOKOLOID SILIKA MENGUNAKAN PENDEKATAN PEMBENTUKAN MISEL

ABSTRAK

Nanopartikel (NPs) silika koloid telah disintesis dengan menggunakan pendekatan pembentukan misel. Kaedah ini sangat bermanfaat bagi menghasilkan NPs silika taburan sekata dengan pelbagai saiz dari 20-160 nm dengan mengubah suhu tindak balas dan jumlah pelarut bersama 2-butanol. Surfaktan bukan ionic Tween 80 telah digunakan untuk membentuk struktur misel bagi memerangkap ubat dan secara langsung membantu dalam pembentukan NPs silika sfera koloid. Berbanding dengan kaedah lain, kaedah ini menawarkan proses memuatkan ubat yang mudah di mana molekul ubat akan terus terperangkap di dalam struktur misel sebelum NPs silika terbentuk. Dalam kerja ini, hanya sejumlah kecil surfaktan telah digunakan tanpa perangkap tambahan. Selain itu, kadar kejayaan memerangkap ubat di dalam NPs silika sangat memberangsangkan dengan penyingkiran surfaktan telah dilengkapkan dengan proses dialisis yang tidak menjejaskan sifat-sifat NPs silika koloid. Jumlah optimum Si prekursor (VTMS) adalah 2 ml. Meningkatkan jumlah Si prekursor akan menghasilkan taburan bimodal. Dua ubat Tuberculosis, Isoniazid (larut air) dan Rifampicin (kurang larut air) telah dipilih sebagai model ubat. Kestabilan 50 nm dan 70 nm NPs silika dengan ubat Rifampicin terperangkap (SiRIF) di dalam NaCl dan serum tikus dengan pelbagai kepekatan telah diuji. Profil pelepasan 50 nm dan 70 nm SiRIF di dalam pelbagai kepekatan PBS dan pH (1.4, 6.8 dan 7.4) telah dibandingkan. 70 nm SiRIF menunjukkan pelepasan yang perlahan (31%) berbanding dengan 50 nm SiRIF (44%) selama 5 hari. Keputusan IC₅₀ dari ujian ketoksikan WST-1 ke atas sel-sel osteosarcoma menunjukkan kebergantung terhadap saiz di mana nanopartikel kecil membawa kepada ketoksikan yang lebih tinggi.

SYNTHESIS OF SILICA NANOCOLLOIDS DRUG DELIVERY SYSTEM (DDS) BY MICELLE FORMATION APPROACH

ABSTRACT

Silica nanoparticles (NPs) colloids were synthesized by using the micelle formation approach. This method was beneficial to produce monodispersed silica NPs with 20 nm to 160 nm size range by varying the reaction temperature and volume of co-solvent 2-butanol. Non-ionic surfactant Tween 80 was used to form micelles structure to entrapped drug and directly assists in the formation of sphere silica NPs colloids DDS. Compared to other methods, this method offers an easy process of drug loading whereby the drug molecules are directly entrapped inside the micelle structure before the formation of silica NPs. In this work, a small amount of surfactant was used without additional functionalizer. Besides, the success rate of drug entrapment in silica NPs was promising with removal of surfactant was completed by dialysis process which did not affect the properties of colloidal silica NPs. The optimum volume of Si precursor (VTMS) is 2 ml. Increase amount of Si precursor formed bimodal distribution. Two Tuberculosis drug, Isoniazid drug (water soluble) and Rifampicin drug (poor water soluble) were chosen as drug model. Stability of 50 nm and 70 nm silica NPs with entrapped Rifampicin drug (SiRIF) in various concentration of Sodium Chloride (NaCl) solution and mouse serum volume percentages were tested. Release profile of 50 nm and 70 nm SiRIF in various Phosphate buffer solution (PBS) and pH (pH 1.4, pH 7.4 and pH 6.8) were compared. 70 nm SiRIF showed slower release (31 %) compared to 50 nm SiRIF (44 %) for 5 days. IC₅₀ results from toxicity test WST-1 assays on osteosarcoma cells showed size dependent whereby smaller nanoparticles lead to higher toxicity.

CHAPTER 1

INTRODUCTION

1.1 Research background

Nanotechnology is a technology using nanosize matter (1-100 nm) that can be developed into devices and systems (Provenzale & Silva, 2009). The use of nanotechnology in medical application has been developed into a promising research area known as nanobiotechnology (Ahmed *et al.*, 2012). The application of nanomaterials in medical field is very much welcomed especially in theranostic application. The main advantage of using nanomaterials is that its properties can be tuned or manipulated in order to meet the specific requirements of particular applications (Sumer & Gao, 2008).

Recently, a lot of effort and attention are focusing on developing drug delivery system (DDS) based on nanotechnology because it is promising for targeted delivery to tissue of interest (Mamaeva *et al.*, 2012). DDS is a system that is capable of carrying agents and releasing them at a specific targeted area with a specific rate. The main objective of such systems is to control the dosage concentration and duration of drug administration without harming the patient while treating the patient's health (Mishra *et al.*, 2010, Mamaeva *et al.*, 2012). The nanoparticles use in DDS must have characteristics such as biocompatible, stable in biological media, able to achieve high loading drug molecules, potential to be used in both hydrophilic and hydrophobic molecules, long circulation in blood, improve drug bioavailability, able to control the drug release and low toxicity (Barbe *et al.*, 2004, Diab *et al.*, 2012, Koo *et al.*, 2005, Mathuria, 2009, Ochekpe *et al.*, 2009, Provenzale & Silva

2009). The candidates for DDS that have been intensively studied are polymeric micelles, polymer-based nanoparticles, lipid based nanoparticles (liposomes), dendrimers, magnetic nanoparticles, metals and inorganic nanoparticles (des Rieux *et al.*, 2006, Kedar *et al.*, 2010, Koo *et al.*, 2005, Lawrence & Rees, 2012, Mishra *et al.*, 2010).

Ceramic (inorganic) nanomaterials have advantages of high mechanical strength, good chemical stability, biocompatible, and resistance to microbial attack as compared to their organic (polymeric) counterparts (Rosenholm *et al.*, 2010). Silica is a member of ceramic family that has potential to be used in biomedical applications such as DDS, biosensors, biomarkers, enzyme supporters etc. (Cellesi & Tirelli, 2006, Klichko *et al.*, 2009, Santra *et al.*, 2001). Silica based DDS has been widely studied because of its interesting properties such as well defined structures and surface properties appear to be a promising candidate as a DDS material. Silica is a very appealing material for DDS because it is relatively inexpensive, and chemically and thermally stable (Gadre & Gouma, 2006). Silica also offers the properties needed for nanoparticles based DDS such as low toxicity, biocompatible, high surface area, hydrophilic and porous structure that are useful for tailoring the encapsulation of drugs or any biomolecules (Chen *et al.*, 2012, Fuertes *et al.*, 2010, Thomas *et al.*, 2010).

Different types of silica have been studied as DDS such as mesoporous silica, silica aerogel and xerogel, sol gel-based silica, hollow silica, core-shell silica, colloidal silica and hybrid silica (Huang *et al.*, 2011, Korteso *et al.*, 1999, Liu *et al.*, 2011, Rosenholm *et al.*, 2009, Slowing *et al.*, 2007, Yang *et al.*, 2008, Yunos *et al.*,

2009, Zhou *et al.*, 2010). There are a lot of methods to synthesis silica nanoparticles (silica NPs) for instance Stöber method, ionic liquid template, hydrothermal, microemulsion, reverse micelles/micelles (Finnie *et al.*, 2007, Ghosh *et al.*, 2012, Liu *et al.*, 2006, Nozawa *et al.*, 2005). All of these methods used sol-gel basic concept whereby hydrolysis and polymerization reaction processes are applied in different system (Nakazaki *et al.*, 2008).

1.2 Problem statement

Synthesis of silica NPs can be achieved by various methods such as conventional sol-gel method, microemulsion method and hydrothermal method. However, some of these methods have some limitations such as produce big size particles, particles agglomeration and complexity during washing and drying process (Andrade *et al.*, 2013, Ganguly *et al.* 2010). Furthermore, the state of end product is in powder form which is only suitable as oral DDS (Kim *et al.* 2010). However, these methods are unsuitable to produce colloidal silica NPs which can be administered by different paths such as oral, parental, transdermal or by intravenous (IV) (Lawrence & Rees, 2012). In this work, silica NPs colloids was produced by combining sol-gel process with emulsion method whereby surfactant micelles acted as a structure template and indirectly facilitate in loading of drug molecules.

There are a lot of hydrophobic drugs and not stable which make the administration of naked drug fail and ineffective. The limitations of the naked drug systems are their limited chemical and mechanical stability in biological condition and extreme condition. In addition, naked drugs also susceptible to microbiological contamination. In fact, inadequate control over drug-release rate also could lead to

ineffective drug administration (Rosenholm *et al.*, 2010). Besides, the incompetent of other carriers like polymeric materials make silica NPs colloids DDS as an excellent candidate for drug carrier. Polymeric materials only suitable for fast release instead of sustained release and easily agglomerate in biological media (Lin *et al.*, 2012, Vaishali *et al.*, 2010).

Several reported works have produced silica NPs DDS via absorption after silica NPs powder is produced (Andrade *et al.*, 2013, Charnay *et al.*, 2004, He *et al.*, 2010, Thomas *et al.*, 2010, Zhang *et al.*, 2010). Zhang *et al.* (2010) and He *et al.* (2010) immersed the silica NPs powder into drug solution to load drug into mesoporous structure of silica NPs. The weaknesses of this approach are unable to control the amount of drug absorb into the silica and could cause a fast release (He *et al.*, 2010, Zhang *et al.*, 2010). Other than that, reverse micelles formation also has been used to synthesize silica NPs DDS. Unfortunately drugs or molecules with poor water solubility have limitations in reverse micelles system (Abarkan and Doussineau, 2006, Bagwe *et al.*, 2004). Research on direct drug impregnation into silica during synthesis is limited. Most researchers tend to load drugs after synthesis and focus more on pore structure and sizes (Parida *et al.*, 2006, Santra *et al.*, 2001). Some studies also have added functionalizers to link the molecule with silica NPs (Bagwe *et al.*, 2004, Min *et al.*, 2005).

In this work, the problems of previous reported works could be overcome by synthesized silica NPs colloids using the micelles formation approach. In this method, a small amount of surfactant was used without additional functionalizer. Besides, the success rate of drug entrapment in silica NPs is promising with complete

removal of surfactant was carried out via dialysis process. This method offers an easy process of drug loading whereby the drug molecules are directly entrapped inside the micelle structure before formation of colloidal silica NPs. Silica NPs colloids entrapped Rifampicin (SiRIF) with uniform particle size distribution can be controlled by varying the synthesis parameters such as reaction temperature, amount of surfactant, butanol volume, and drug loading concentration. In addition, stability of SiRIF in salt solution and biological media (NaCl and mouse serum) is also examined to assess the performance of SiRIF as drug carrier. Moreover, drug release properties are systematically studied by varying the concentration of phosphate buffer solution (PBS) and its pH.

1.3 Objectives

The main objectives of this research are:

- i. To synthesis and characterize silica NPs colloids for drug delivery system.
- ii. To optimize entrapment of silica NPs colloids with Tuberculosis drug.
- iii. To study stability of silica NPs colloids with drug in biological media.
- iv. To study release properties of silica NPs colloids as drug delivery system.

1.4 Thesis scope

This dissertation consists of five chapters. Chapter 1 discusses on the research background, problems statement and objectives of the research. Literature review of related works is discussed in Chapter 2. While in Chapter 3, experimental details and characterization used are explained in details. In Chapter 4, the results and discussions of this research are presented. Finally, conclusion and recommendations for future work are stated in Chapter 5.

CHAPTER 2

LITERATURE REVIEW

2.1 Introduction

Nanotechnology can be defined as development of materials and devices in nanometer scales (1-100 nm) which involves fundamental understanding of physical properties of nanomaterials (Koo *et al.*, 2005). Nanotechnology also has expand recently whereby nanoparticles based materials have been applied in biological applications such as diagnostic, bioimaging, gene transfer and drug delivery owing to their properties such as high surface area and size dependent qualities (Chang *et al.*, 2007, Tan *et al.*, 2004). Drug delivery system (DDS) is a system that delivers the pharmaceuticals or therapeutics molecules to a target or organ of interest.

Conventional DDS usually administers drug by oral route which initiates an early release of drugs (Strømme *et al.*, 2009). Nanoparticles based DDS could improve the conventional DDS by boosting the infiltration of the therapeutic molecules into blood barriers and prolong the transmission of drugs (Lopez *et al.* 2009, Wanyika *et al.*, 2011). DDS based on colloidal silica NPs is favourable because it is biocompatible, biodegradable, spherical shape, unique surface properties, tunable size and stable from aggregation (Fuertes *et al.*, 2010, Guo *et al.*, 2008, Wang, 2009).

2.2 Silica nanoparticles (NPs)

Silica is one of the abundant earth's crust which also exists in biological system (An *et al.*, 2010). Synthetic amorphous silica has gained attention in the nanobiotechnology especially DDS. The properties such as tunable porosity, biocompatible, biodegradable, low toxicity and resistant in extreme environment make silica as a potential candidate for DDS (Nampi *et al.*, 2012). There are three main types of silica which are all found under CAS No. 7631-86-9 as shown in Figure 2.1, (1) crystalline silica, (2) amorphous silica (naturally occurring or as a by-product in the form of fused or fumed silica), and (3) synthetic amorphous silica, including silica gel, precipitated silica, pyrogenic (fumed) silica and colloidal silica (sol) (Fruijtier-Pölloth, 2012). The difference between the amorphous and crystalline silica lies in the arrangement of the tetrahedral units. The arrangement of tetrahedral units for amorphous silica is random, whereby all oxygen at the corners are bonded with two nearby tetrahedra. Although there is no long range periodicity in the network there remains significant ordering at length scales well beyond the silica bond length (Fruijtier-Pölloth, 2012).

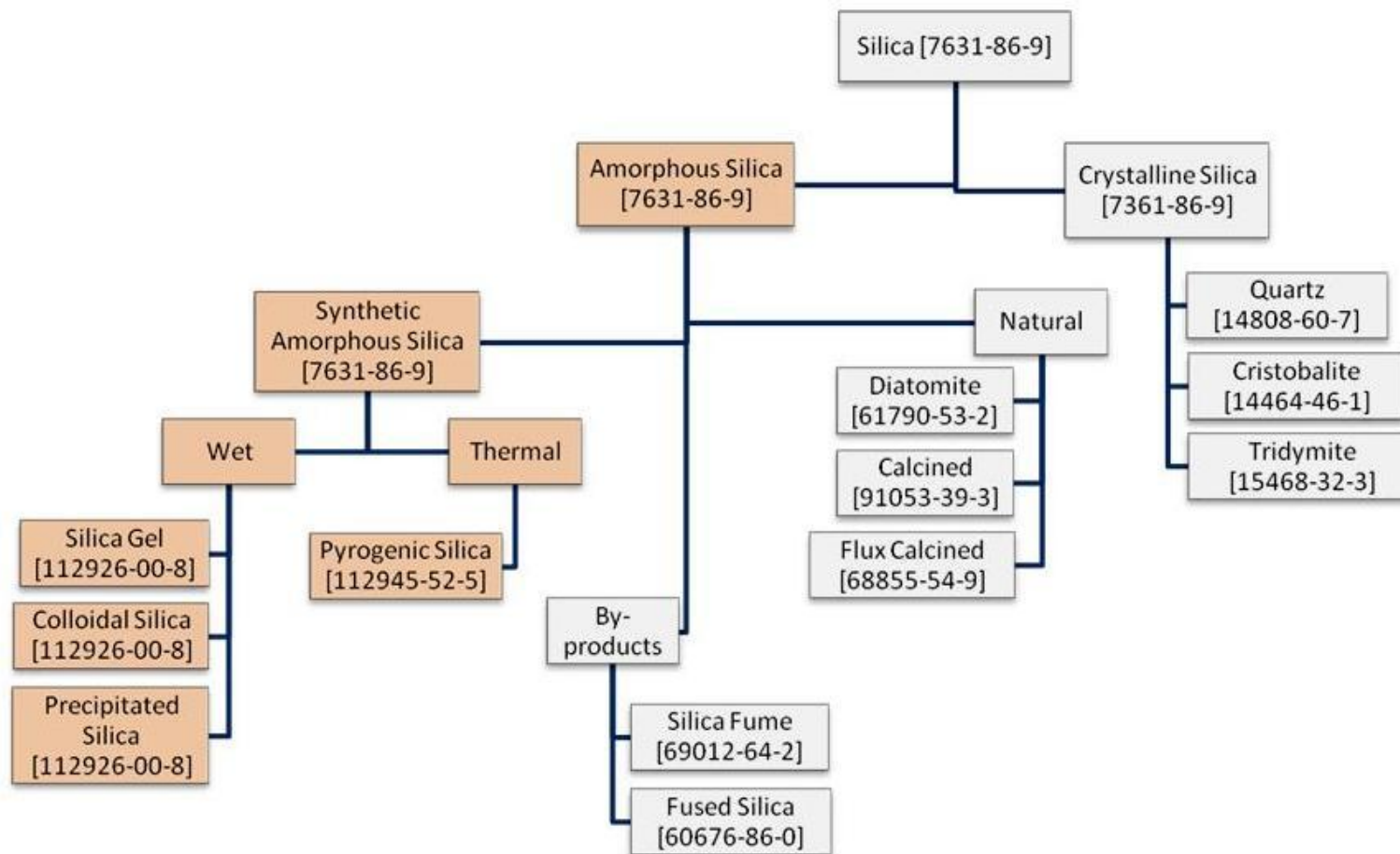


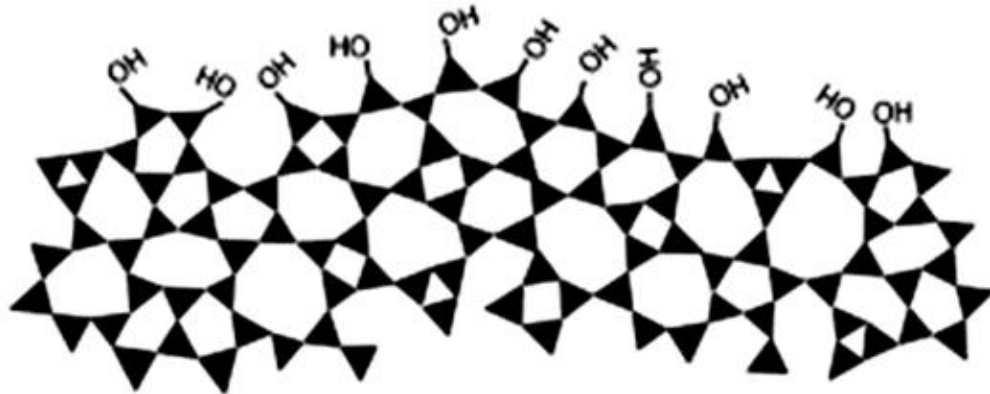
Figure 2.1: Various forms of silica (Fruijtier-Pölloth, 2012)

2.2.1 Properties of Silica

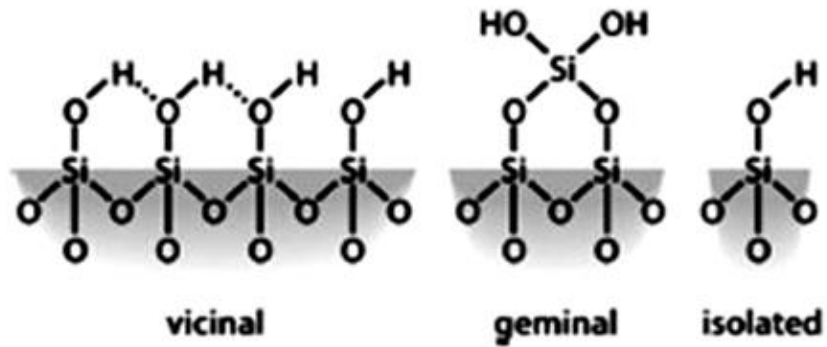
There are several ways to produce amorphous silica. Fumed or pyrolytic silica can be produced by pyrolysis process which uses high temperature (1200-1400 °C). In addition, colloidal, precipitates and mesoporous silica can be produced using hydrolysis and condensation reactions in aqueous solution or using hydrothermal process (Zhang *et al.*, 2012). Unlike crystalline silica, amorphous silica has short-range order and its structure is strongly dependent on kinetic and environmental factors because of a weak energy site. Schematic diagram in Figure 2.2 shows how amorphous silica structure is built from the siloxane framework architecture, which consists of combination of closed siloxane rings (Figure 2.2, Scheme 1), along with the concentration, pattern, and extent of hydrogen bonding of silanol groups ($=\text{Si}-\text{OH}$) that terminate the siloxane rings at the silica surface (Figure 2.2, Scheme 2). Silica could contain relatively high concentration of surface-associated radicals (Figure 2.2, Scheme 3) as it has high surface area (Zhang *et al.*, 2012).

Water adsorbs preferentially on the residual silanols which can be divided into three groups: isolated silanols, geminal silanols and vicinal silanols on the siloxanes. The most active silanol group is geminal silanols but their concentration on the surface is the lowest (10–12 %). Isolated silanols concentration is the highest (60–65 %), while vicinal silanols on the siloxanes (Si-O-Si) make the rest (Buszewski *et al.*, 2012). Table 2.1 lists physical and chemical properties of different types of amorphous silica like pyrogenic, precipitated and colloidal silica (Fruijtier-Pölloth, 2012).

Scheme 1. Schematic depicting the ring structure of amorphous silica and the amorphous silica surface after equilibration with hydroxyl groups



Scheme 2. Types of silanol groups that can exist on the amorphous silica surface



Scheme 3. Radicals that can exist on the amorphous silica surface

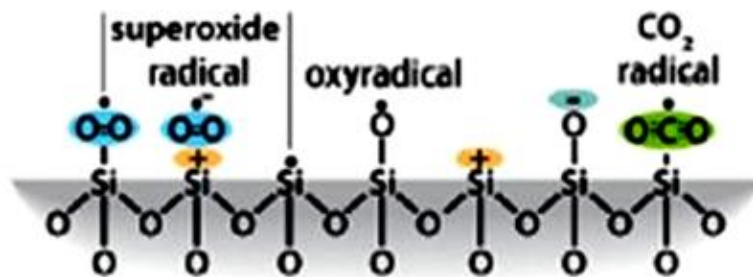


Figure 2.2: Schematic diagrams of amorphous silica structures and reaction on its surface (Zhang *et al.*, 2012).

Table 2.1: Physical and chemical properties of different amorphous silica (Fruijtier-Pölloth, 2012).

Property [units]	Pyrogenic	Precipitated	Colloidal
Space group	Not measurable for amorphous materials		
SiO ₂ content [wt%]	≥ 99.8	> 95%; gel:>95% (dry)	≥ 99.5
Loss of drying [%]	< 2.5	5-7; gel: 2-6	>> 2.5
Melting point [°C]	1600-1725	1600-1725	1600-1725
Density (g/cm ³ at 20 °C)	2.2	2.2	2.2
Water solubility (saturation) [mg/L] at 37 °C and pH 7.1-7.4	144-151: (15-68 at 20 °C and pH 5.5-6.6)	141; gel: 127-141	Colloidal dispersion in water
Specific surface area (SSA)	50-400	30-500; gel: 250-1000	50-380 (spherical) ~640 (porous)
Zeta potential	Negative	Negative	Usually negative, can be positive with certain stabilizer
Behavior towards water	Hydrophilic	Hydrophilic	Hydrophilic
Porosity	Microporous	Meso- or macroporous	-

2.2.2 Structure of Silica NPs

There are various types of silica structure that can be produced by manipulating the synthesis parameters as shown in Figure 2.3. Silica also can be classified according to its shapes such as mesoporous silica spheres, nanorods and nonporous silica like Stöber silica or hollow silica. Mesoporous silica is a common silica that has 2-50 nm pore size range. There are several mesoporous silica that can be classified according to their pore structures. The most common mesophases in mesoporous silica with pore size between 2 and 5 nm are 2D hexagonal p6m, 3D cubic Ia3d and lamellar p2 which are related to MCM-41, MCM-48 and MCM-50

(Mobil Catalytic Material Number 41, 48 and 50) materials, respectively. For silica with larger pore size (6 to 20 nm wide) the 2D hexagonal $p6mm$ structure is the most commonly reported for SBA-15 (Santa Barbara Amorphous-15) (Slowing *et al.*, 2010). Silica nanorods with different length and porosities can be produced by modifying the primary amine silane groups as shown in Figure 2.3 (Yu *et al.*, 2011).

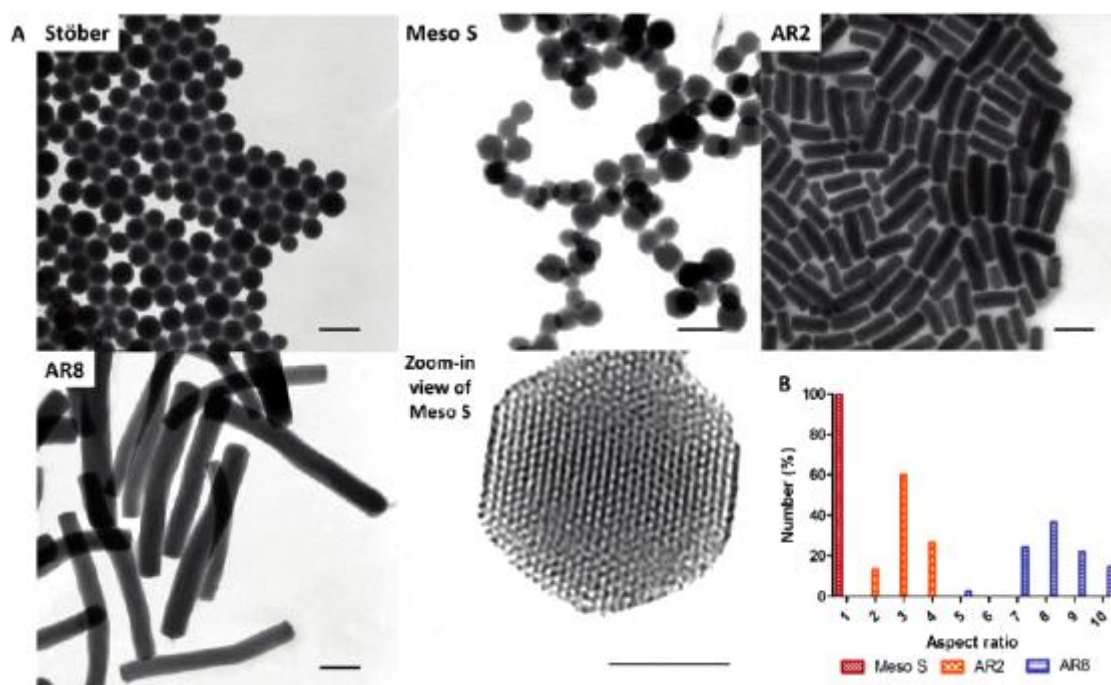


Figure 2.3: (A) Transmission electron microscope (TEM) images of nonporous silica (Stöber), mesoporous silica (Meso S), mesoporous silica nanorods with aspect ratio 2 (AR2), and mesoporous silica nanorods with aspect ratio 8 (AR8) and High resolution TEM (HRTEM) image of a nanoparticle from Meso S; scale bars = 200 nm except in high-resolution image = 50 nm (Yu *et al.*, 2012)

Nonporous silica like Stöber silica usually in colloidal forms (Hartlen *et al.*, 2008). Compared to other silica microstructure, this type of silica has a good monodispersity. The different of nonporous silica with porous silica lies in the final synthesis process. Porous silica is subjected to washing, filtering and calcination

process, while nonporous silica is maintained in colloidal form. Wang *et al.* (2010) synthesized porous silica hollow spheres by leaching the porous nickel silicate hollow spheres (Wang *et al.*, 2010). While, Chen *et al.* (2004) have used calcium carbonate (CaCO_3) as a template that was removed by dissolved in hydrochloric acid (HCl) solution. Manipulation of the synthesis parameters can tune the size and shell thickness of porous hollow silica spheres. Other researchers also have reported on using polystyrene (PS) as a template (Fu and He, 2011, Kato *et al.*, 2010).

2.2.3 Silica surface properties

Silanol groups can form on the silica surface by two processes. First, during synthesis process, whereby condensation and polymerization of silicic acid ($\text{Si}(\text{OH})_4$) occurs (Figure 2.4 (a)). Here, the reaction solution becomes supersaturated and transform into polymeric form. Then, it changes to colloidal containing spherical particles where silanol ($\text{Si}\equiv\text{OH}$) groups are present on the surface. However, concentration of silanol group presents on silica surface depends on the final state of silica itself either in colloids, gels or powder. Drying or applying heat treatment on the silica will produce silica gel or silica powder, which only contains some of the silanol groups on its surface because of water molecules, is removed. Secondly, in the present of water or aqueous solutions, the surface hydroxyl (OH^-) groups are formed because of the rehydroxylation of dehydroxylated silica.

The free valence electron becomes saturated with hydroxyl groups in an aqueous medium (Figure 2.4 (b)) because Silicon atoms tend to complete the tetrahedral formation on the surface. There are several types of hydroxyl (OH^-) groups on the surface such as (1) isolated free (single silanols), $\equiv\text{Si}-\text{OH}$; (2) geminal

free (geminal silanols or silanediols), $=\text{Si}(\text{OH})_2$ which is bonded by hydrogen bond (H-bonded single silanols, H-bonded geminals, and their H-bonded combinations) (Figure 2.5). On the silica surface also exists siloxane groups where the $\equiv\text{Si}-\text{O}-\text{Si}\equiv$ bridges are formed with oxygen atoms on the surface. Also, there is structurally bound water inside the silica skeleton and very fine ultramicropores, $d < 1\text{nm}$ (d is the pore diameter), i.e. internal silanol groups (Zhuravlev, 2000).

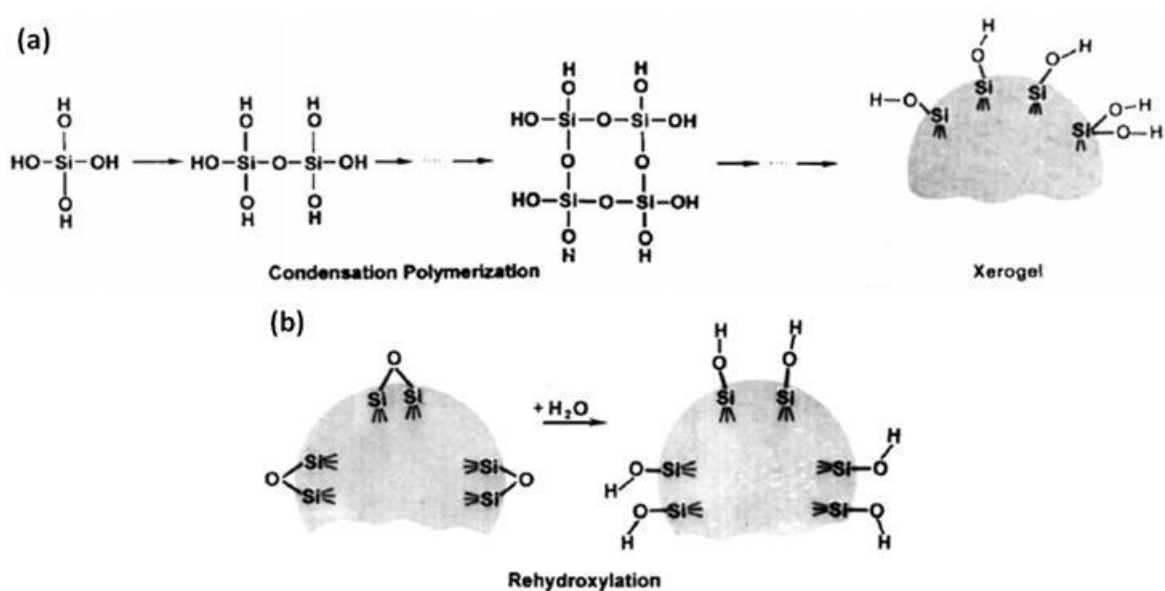


Figure 2.4: The formation of silanol groups on the silica surface: (a) Condensation polymerization; (b) Rehydroxylation (Zhuravlev, 2000)

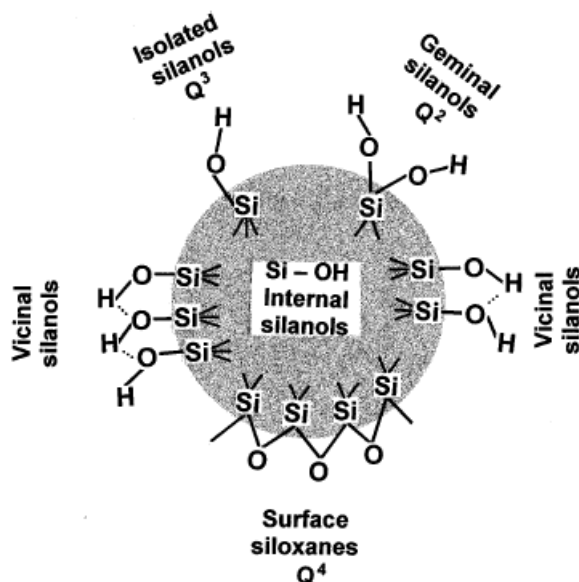


Figure 2.5: Types of silanol groups and siloxane bridges on the surface of amorphous silica, and internal (OH⁻) groups. Qⁿ terminology is used in NMR, where n indicates the number of bridging bonds (-O-Si) tied to the central Si atom: Q⁴, surface siloxanes; Q³, single silanols; Q², geminal silanols (silanediols) (Zhuravlev, 2000)

2.2.3.1 Adsorption of organic molecules on silica surface

Several organic molecules can be attached on the surface either by chemical bonding, hydrogen bonding, hydrophobic bonding or Van der Waals force to unique properties of silica surface (Parida *et al.*, 2006). Cationic and nonionic surfactants are adsorbed on silica surface with hydrogen bonds. Sometimes, adsorption process of surfactants also is contributed by the polar part of surfactant itself. When silica surface is modified with alkali, the adsorption behaviour of cationic surfactant or polyethylene glycol changes due to changes in the characteristics of silica or modified silica surface. Cationic adsorption on silica in salt solution can be by electrostatic interaction with the alkyl tails and hence produces hydrophobic surface properties (Wang & Gu, 2005). Generally, nonionic surfactants have short hydrophilic oligo-oxyethylene headgroups that is relative to the size of the

hydrophobic tail and able to form bilayers and micellar structures on adsorption on surfaces of micellar structures. Sharma *et al.*, (2010) reported that the adsorbed nonionic surfactant micelles provides steric repulsion between the particles which provides stability against aggregation.

Polymers have polyfunctional groups that can attract to the hydroxyl groups of silica surface and hence can undergo adsorption. The adsorption of polymers depends on various factors such as the structure of polymer, surface structure, pH of the medium, temperature and the geometry of adsorbate (Yagüe *et al.*, 2008). Polyethylene glycol (PEG) is a hydrophilic polymer that bond to silica through esterification on silica hydroxyl groups and silanol groups or attach by hydrogen bonding on the external surface of silica. Yagüe *et al.* (2008) and Yu *et al.* (2003) reported that adsorption of PEG could decrease adsorption of protein and consequently increases the particles circulation half time (Yagüe *et al.*, 2008, Xu *et al.*, 2003).

Hydrophobic and hydrophilic binding sites of silica have been studied by adsorptions of some natural biomolecules such as proteins. Proteins have heterogeneous surface which can be positively or negatively charged. Silica with negative charge surface tends to have ionic properties with both hydrophilic (silanol groups) and hydrophobic surfaces. Hence, human serum protein (HSA) has nonspecific binding to silica by ionic attraction, hydrogen-bonding and non-polar (He, Zhang, *et al.*, 2010). In a biological condition, the surfaces of nanomaterials can be modified by the adsorption of biomolecules that causes the formation of particle–corona complex. The formation of a corona layer on the silica surface inhibits

cytotoxicity and hemolysis (Shi *et al.*, 2012). Adsorption of some biomolecules like lysozyme and albumin is dependent on pH. Usually, the adsorption process occurs due to electrostatic interaction between adsorbate and adsorbent (Parida *et al.*, 2006).

2.2.3.2 Surface functionalization of silica

Surface of silica can be modified by adding functionalize group on its surface in order to improve the surface properties especially to achieve minimum nanoparticles aggregation and reduces nanoparticles nonspecific binding. The surface can be modified either by mechanical, physical, chemical or biological functionalization (Hildebrand *et al.*, 2006). There are three main ways for functional groups to be attached to the silica surface: reaction between organosilanes or organic molecules with silica surface functions, chlorination of the silica surface followed by reaction of the Si–Cl with an appropriate functional molecule, or by incorporation of functional groups via sol–gel methodology followed by post-modification (Dash *et al.*, 2008).

2.3 Synthesis and fabrication of Silica NPs

Silica NPs can be produced by various methods starting from synthesis process until drying process which can end as different product. Figure 2.6 shows different process to produce different morphology and types of silica (Napierska *et al.*, 2010).

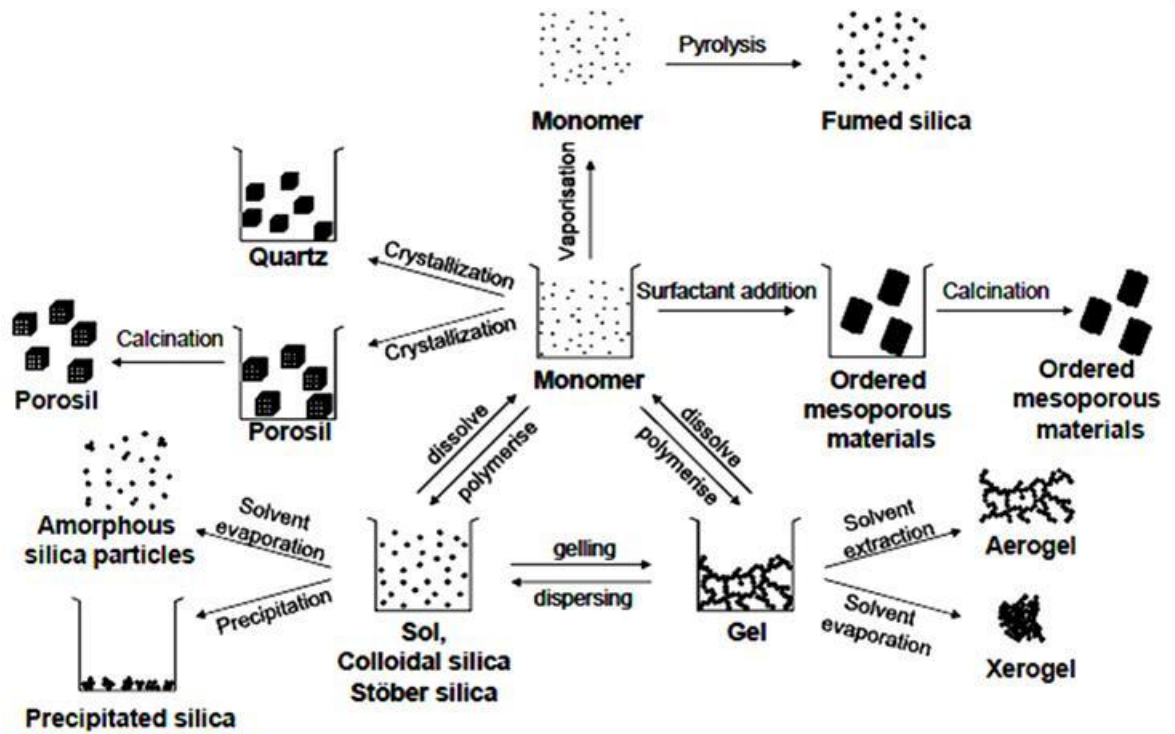


Figure 2.6: General schematic diagram of silica synthesis processes (Napierska *et al.*, 2010)

2.3.1 Sol-Gel process

The sol-gel process is a wet-chemical method which has been widely used in producing metal oxides or ceramic materials (Rahman & Padavettan, 2012). The process starts from a colloidal solution called sol that acts as the precursor for formation of gel like aerogel or xerogel (after drying) depending on solvent removal process as shown in Figure 2.7 (Morosanova, 2012). The Si precursor undergoes hydrolysis and condensation reactions in the presence of water and alcohol as co-solvent. Hydrolysis occurs and hydroxyl ions attach to Si precursor and produce alcohol as byproduct (equations 2.1 and 2.2). While, condensation occurs when silanol groups form siloxane bridge and release water and alcohol as byproducts (equations 2.3 and 2.4) (Gadre and Gouma, 2006, Radin *et al.*, 2001).

Hydrolysis in water:



Condensation in water:



Condensation in alcohol:

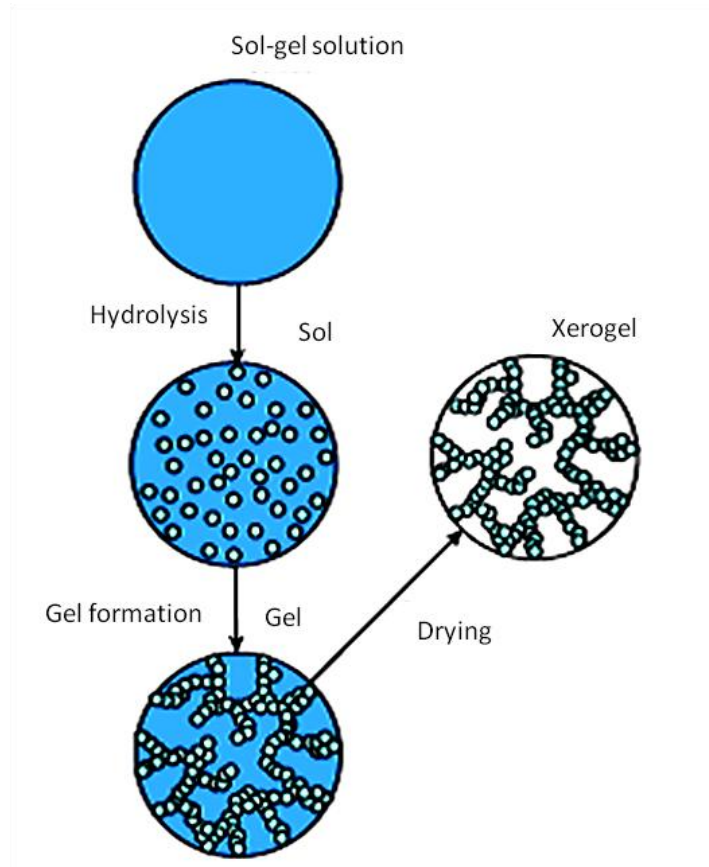


Figure 2.7: The stages of silica sol-gel materials synthesis (Morosanova, 2012)

Through sol-gel process, monodispersed silica particles with sizes ranging from nanometer to micrometers can be produced by different synthesis approaches

such as microemulsion, Stöber method, ionic liquid template and hydrothermal method. All of these methods require extremely diluted reactions solutions (Kim *et al.* 2010). Silica NPs produced by the conventional sol-gel method usually have irregular morphology and slightly agglomerate. This condition is due to drying process especially to produce powder form silica. Besides, drying process to remove the water produces two different silica gel. Silica aerogel can be produced using a supercritical drying of the wet silica gel in an autoclave. While, silica xerogel is dried at ambient temperature which is much simpler and safer. Silica xerogel produced is denser compared to silica aerogel due to shrinkage of particles during drying process (Håreid *et al.*, 1996). On the other hand, Lindberg *et al.*, (1995) have studied sol-gel silica NPs by varying synthesis parameters such as temperature, mixing and salt addition whereby monodispersed silica NPs from 50 to 700 nm were produced.

2.3.1.1 Stöber process

The Stöber process involves physical and chemistry processes to synthesis monodispersed silica NPs. The process was discovered by G.Kolbe in 1956 and redeveloped by Stöber *et al.* in 1968 (Tabatabaei, 2006). Usually tetraethyl orthosilicates (TEOS) as precursor is added into a large amount of water mixed with a low molar-mass alcohol solvent such as ethanol or methanol. Typically, this process is aided by catalyst either in basic or acidic condition. This method can produce monodispersed silica NPs with size varying between 50-2000 nm depending on types of precursor, alcohol and volume ratio of reactant with water (Nozawa *et al.*, 2005). It also can produce particles size up to 1 μm which has been reported in a modified technique (Lindberg *et al.*, 1995). Nozawa *et al.* (2005) also have reported that particle size can be varied by using the seeded growth method where up to 2 μm

monodispersed silica can be produced by varying the precursor addition rate and stirring rate.

There are two paths of formation of monodispersed particles in Stober method either by LaMer mechanism or based on thermodynamic stabilization of particles (Guo *et al.*, 2008). Lamer mechanism suggests that nucleation is the limiting factor in the growth process, whereby a constant number of nuclei further grows with increasing the precursor concentration (Malik *et al.*, 2010). Meanwhile, for thermodynamic stabilization of particles, the nuclei forms continuously during the reaction and starts to aggregate with each other forming bigger particles. Guo *et al.* (2008) have synthesized monodispersed silica with size 10-100 nm by using the two-stage process (seed and growth) and regrowth approach of basic elemental silica precursor like TEOS, tetramethyl orthosilicate (TMOS) and tetrapropyl orthosilicate (TPOS).

Figure 2.8 shows the monodispersed silica NPs produced using the regrowth of seed using TEOS precursor which the size of silica NPs can be increased by regrow the seed up to five times (Guo *et al.*, 2008). Hartlen *et al.*, (2008) also have produced monodispersed silica particles with size range 15-200 nm using the regrowth approach and arginine as the base catalyst. Yokoi *et al.* (2009) also have synthesized smaller silica with size range 8-35 nm based on the Stöber method but with different catalyst instead of ammonia which are arginine and lysine. This weak base induces slow hydrolysis process instead of fast hydrolysis process in the conventional Stöber method (Yokoi *et al.*, 2009).

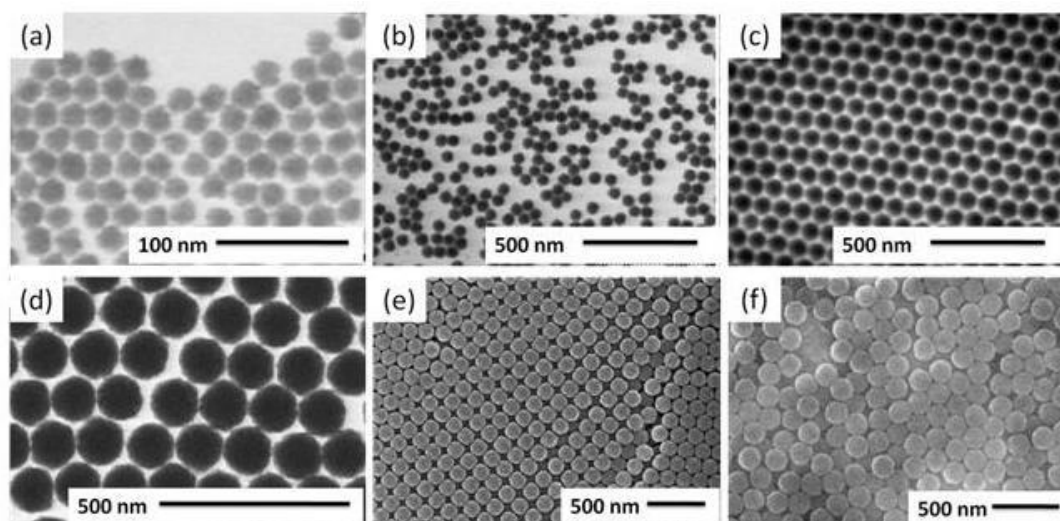


Figure 2.8: Electron microscopy images of monodispersed silica NPs with various size ranges; (a) seed 18.5 ± 0.8 nm produced by the single stage growth, (b) the one stage regrowth seed 45.5 ± 1.3 nm, (c) the two stage regrowth seed 84 ± 2 nm, (d) three stage regrowth seed 117 ± 2.5 nm, (e) the four stage regrowth seed 141 ± 2.5 nm and (f) the five stage regrowth seed (Guo *et al.*, 2008)

2.3.2 Hydrothermal growth method

Hydrothermal is a process that occurs either in single- or heterogeneous phase reaction in aqueous solution at temperature higher than room temperature and under pressure higher than 100 kPa (Ugheoke & Mamat, 2012). The process usually is carried out in a sealed container such as Teflon coated autoclave (Kim *et al.*, 2010). During the synthesis process, the volatile organic solvent and byproducts like alcohol and water are evaporated from the system (Wei *et al.*, 1999). The interaction between the Si precursor and the surfactant template introduced stabilizes the silica framework and prevents it from collapse caused by pressure and internal stress during the drying process. Several works have synthesized silica NPs using the hydrothermal growth method by varying the synthesis parameters such as temperature, amount of surfactant, types of organic solvent and hydrothermal time (Kim *et al.*, 2010, Ganguly *et al.*, 2010, Carrillo *et al.*, 2011, Hu *et al.*, 2011).

Conventional hydrothermal synthesis produces larger particle size which is around 1 μ m (Kim *et al.*, 2010). However, in the recent works surfactant template was introduced to control the particle size and the pore structure of particles (Kim *et al.*, 2010, Ganguly *et al.*, 2010, Carrillo *et al.*, 2011). Hydrothermal method is less favourable to produce silica NPs because it uses high temperature, expensive set up, and particles produced are big and sometimes form irregular shape compared to other methods (Kim *et al.*, 2010, Hu *et al.*, 2011). But this method can produce silica particles with bigger pore size (Hu *et al.*, 2011, Ganguly *et al.*, 2010). Figure 2.9 shows different surfactant used in hydrothermal growth method, whereby each surfactant produces silica NPs with different pores sizes. Sodium lauryl sulfate (SLS) surfactant produces large particles size distribution varies from 20 to 150 nm (Ganguly *et al.*, 2010).

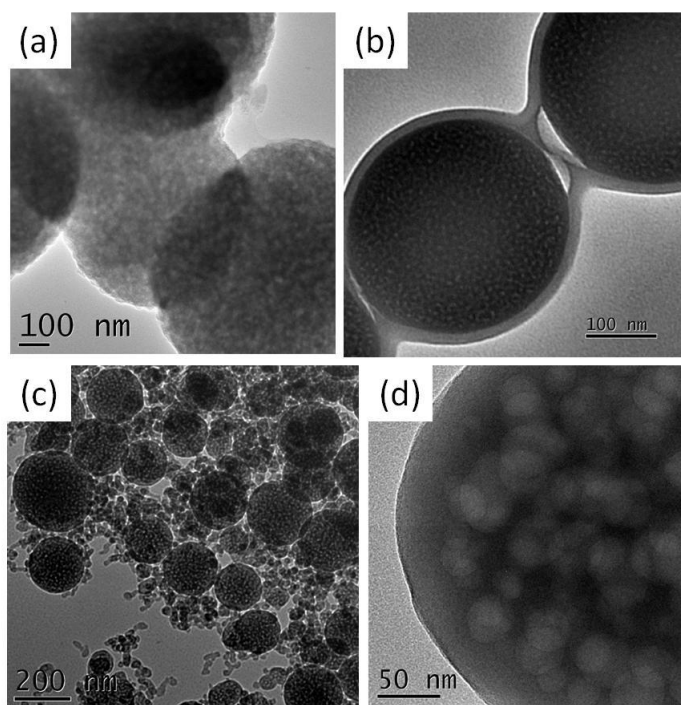


Figure 2.9: TEM images of silica NPs produced by using different surfactants; (a) cetyl trimethyl ammonium bromide (CTAB), (b) Tergitol, (c) Sodium lauryl sulfate (SLS) and (d) polyethylene glycol (PEG) (Ganguly *et al.*, 2010)

2.3.3 Ionic liquid template

Ionic liquids templates method (IL) is a method that involves any salt in liquid form at temperature below 100 °C. Typically, IL comprises of a large organic cation together with an organic or inorganic anion are present (Donato *et al.*, 2008). Recently, room temperature ionic liquid (RTIL) method is favourable because organic salts with low melting points are used. RTIL is often regarded as a replacement for classical traditional molecular solvents due to their excellent properties such as high ionic conductivity, high polarity, negligible vapor pressure, and thermal stability. The greatest advantage of the RTIL is that it can be designed through altering the anions and cations. Therefore, RTIL microemulsion could have potential applications in material synthesis (Trewyn *et al.*, 2004). Compared to conventional sol-gel method, IL offers longer aging time without shrinkage of the gel network.

This technique allows silica aerogel synthesis under mild chemical condition (Dai *et al.*, 2000). Trewyn *et al.*, (2004) reported the synthesis and characterization of series of mesoporous silica NPs (MSNs) materials by using different RTIL templates such as 1-tetradecyl-3- methylimidazolium bromide (C₁₄MIMBr), 1-hexadecyl-3- methylimidazolium bromide (C₁₆MIMBr), 1-octadecyl-3- methylimidazolium bromide (C₁₈MIMBr), and 1-tetradecyloxymethyl-3- methylimidazolium chloride (C₁₄OCMIMCl) which produced various porous structures and morphologies such as spheres, ellipsoids, rods, and tubes as shown in Figure 2.10 (Trewyn *et al.*, 2004). On the other hand, Zhao *et al.* (2009) have synthesized silica with different condition basic and acid using BmimBF₄ ionic liquid